Calibration of Local Magnitude Scale for Colombia

Camilo Muñoz Lopez[*1], Laura Velasquez[1], and Viviana Dionicio[1]

ABSTRACT

New calibration for local magnitude (M_L) was performed for Colombia. The territory was divided into five zones using reported attenuation values for different areas of the country and correlating this information with the mapped lithologies, the absence or presence of volcanic activity, and patterns in the hypocentral locations of seismicity. Seismic data from the Colombian National Seismic Network—Colombian Geological Survey (RSNC-SGC) were used to obtain a total of 81,232 peak amplitudes from 22,816 earthquakes recorded between January 2015 and August 2017. This set of data was incorporated into a linear inversion to calculate the distance-correction functions for each zone. A new methodology is proposed for calculating the base level of the distance-correction function or parameter *c*, using the amplitude values for earthquakes with moment magnitudes (M_w) close to 3 measured at stations at distances close to 100 km. The distance-correction $\log A_0$ functions obtained in this study for the five zones are: Zone 1:$-\log A_0 = 1.245 \times \log(r) + 0.0024 \times r - 2.051$, Zone 2:$-\log A_0 = 1.056 \times \log(r) + 0.0021 \times r - 1.76$, Zone 3:$-\log A_0 = 1.07 \times \log(r) + 0.0013 \times r - 1.531$, Zone 4:$-\log A_0 = 1.241 \times \log(r) + 0.0015 \times r - 2.178$, Zone 5:$-\log A_0 = 0.711 \times \log(r) + 0.0009 \times r - 0.69$, in which r is the hypocentral distance in kilometers. The results of this study are in use in the RSNC-SGC since September 2018. Before using the equations presented here, the values of local magnitude were previously underestimated for the entire Colombian territory. This work allows the calculation of the local magnitude using the largest attenuation changes in addition to decreasing discrepancies with other magnitude types such as M_w and those calculated by international networks.

KEY POINTS

- Arrival amplitudes were used to improve the magnitude calculation for the National Seismic Network of Colombia.
- The Colombian territory was divided into five zones and distance-correction functions were recomputed by zone.
- Results correct earlier magnitude underestimation to improve the match with other catalogs.

INTRODUCTION

To catalog earthquakes without using felt intensities has always been a basic seismological need. Since the work of Richter (1935), the local magnitude scale (M_L) has been used to describe the relative sizes of earthquakes. Originally, Richter used the maximum *Lg* amplitude from Wood–Anderson seismograph records along with a calibration (distance-correction function) to calculate the M_L value.

Local magnitudes have been calculated since the beginning of the Colombian National Seismic Network—Colombian Geological Survey (RSNC-SGC) in 1993; initially, the calibration of Hutton and Boore (1987) for southern California was applied. More recently until September 2018, the calibration of Rengifo and Ojeda (2004) has been used. The result of this work was a single equation for the entire Colombian territory. This formula was calculated with records of 2312 earthquakes from 17 short-period stations and one broadband seismic station. Moreover, Rengifo and Ojeda (2004) proposed a base-level constraint of 1 mm amplitude at 140 km for earthquakes with magnitudes of M_L 3.0. The M_L calculated with this calibration differs from the M_w, estimated by the RSNC-SGC since 2010 (Hanks and Kanamori, 1979), for most events by at least 0.3 and sometimes up to 0.7 magnitude units, with M_w larger than M_L. This bias raises the question as to which of the two types of magnitude has been miscalculated. When the values of M_w calculated by the RSNC-SGC are compared with magnitudes from international agencies, the difference is almost zero. Furthermore, the value of M_w has been confirmed

1. Seismological Network—Servicio Geológico Colombiano, Bogotá D.C., Colombia

*Corresponding author: olimacc92@gmail.com; camilo.gempa@gmail.com

Cite this article as Muñoz Lopez, C., L. Velasquez, and V. Dionicio (2020). Calibration of Local Magnitude Scale for Colombia, *Bull. Seismol. Soc. Am.* **110**, 1971–1981, doi: 10.1785/0120190226

by several methods, using spectral analysis with the SEISAN software (Havskov and Ottemoller, 1999) and with waveform inversions using programs such as ISOLA (Sokos and Zahradnik, 2008) or *W* phase (Kanamori and Rivera, 2008). These results indicate that the discrepancy is associated with the M_L values.

The distance correction (attenuation) for M_L is very dependent on local geological conditions. Therefore, to improve the determination of M_L, specific corrections must be defined for each region where the attenuation of seismic waves is different. Furthermore, local conditions produce amplifications or decreases in measured amplitudes. Such effects are corrected for at each station and are called "station corrections." Taking into account the differences in attenuation will provide a more reliable M_L adjustment, leading to better tracking of the energy released by the seismicity recorded in the Colombian territory.

High-attenuation values have been found to be associated with areas that have high-fracture density, significant occurrence of seismicity, high temperatures, partial fusion of rocks, high presence of fluids and gases (Gao, 1992), and active tectonic zones. Wong (2001) found attenuation to be higher in the volcanic area "Tres Vírgenes, Baja California" in Mexico. He associated this effect with the presence of a geothermal anomaly. On the other hand, Shyam and Tim (2004) studied changes in seismic attenuation with the presence of hydrates, and their results show that the attenuation increases with hydrates saturation.

Many studies of local magnitude calibration have been performed in places such as southern California (Hutton and Boore, 1987), Norway (Alsaker *et al.*, 1991), and Tanzania (Langston *et al.*, 1998), and some local studies in Colombia such as those in Cerro Bravo—Cerro Machín (volcanic complex; Londono, 2015), Paletará (volcano; Londono and Raigosa, 2016), and Valle Medio del Magdalena (sedimentary basin; Londoño and Romero, 2017) have been reported. These studies exhibit different calibrations for different areas. This fact supports our decision to calculate different M_L calibrations for each zone in the Colombian territory.

Other indications regarding the need for this effort include new data available for M_L calibration, the clear discrepancy between M_L and M_w, and the importance of zoning. The purpose of this study is to develop a new M_L calibration that better represents the energy released by an earthquake occurring anywhere in the country.

ZONING FOR M_L CALIBRATION OF THE COLOMBIAN TERRITORY

For very large areas, important differences have been found in the intrinsic attenuation of seismic waves because of variations in the geology. This factor is especially important for Colombia, which is located in the northwest corner of the South American tectonic plate. Here, its convergence with the Caribbean and Nazca plates, which trend northwest and west–east, respectively, produces a complicated set of tectonic regimes. The clearly variable geological settings in these regions suggest that the attenuation of seismic waves may be significantly different.

de Souza and Mitchell (1998) studied the variations of attenuation in South America. They reported high attenuation in the west and northwest along the active margin where the Andean belt is located. The attenuation values decrease toward the east, where the Brazilian shield is located, which is a stable tectonic zone and therefore has low seismicity.

In general, Colombia's geotectonic location is characterized by high-attenuation values (de Souza and Mitchell, 1998). Jiménez (2003) studied the spatial variations in attenuation within Colombia. He found that intrinsic attenuation dominates over scattering, as a result of the subduction of the Nazca plate beneath the South American plate and of the magma chambers located in the central and southern parts of the country. Although such studies report local variability in attenuation, in general, such variations are greater toward the west, center, and south of the country with smaller variability in the north and east.

Ojeda and Ottemöller (2002) performed tomography of the attenuation for Colombia. They and Ugalde *et al.* (2002) reported the highest attenuation values in the central mountain range, linking this effect to the presence of active volcanic systems. Slightly lower values are recorded to the west, where oceanic rocks that are a product of accretion are surfacing and the boundary of the plate convergence is found.

In northern Colombia, Ambeh and Lynch (1993) studied the attenuation in the eastern Caribbean subduction zone and reported low values of attenuation.

The country was divided into regions, taking into account the attenuation values reported in the studies cited previously, and further regional geological characteristics that may affect the attenuation of seismic waves. However, it is important to clarify that the boundaries of the zones represented in Figure 1 are only proposed and that more detailed studies of the spatial variations in attenuation across the entire Colombian territory will allow more consistent zones to be defined.

We divided the Colombian territory into five zones (Fig. 1):

- Zone 1: The western Cordillera and Pacific region is bounded on the west by the subduction of the Nazca plate and on the east by the Romeral fault system, which includes the Cali-Patía and Mistrató fault systems. Southern and northern boundaries are the Colombian political border with Ecuador, and the geomorphological change because of the western mountain range, respectively (see bottom left in Fig. 1). In general terms, this region is defined by igneous and metamorphic rocks. High-seismic attenuation values in this zone are attributed to the subduction of the Nazca plate beneath the South American plate. Sato and Sacks (1989) noted that the attenuation is related to the flow of fluids in partially saturated rocks of the crust.
- Zone 2: The central Cordillera is bounded on the west by the Romeral fault system, which includes the Silvia-Pijao and

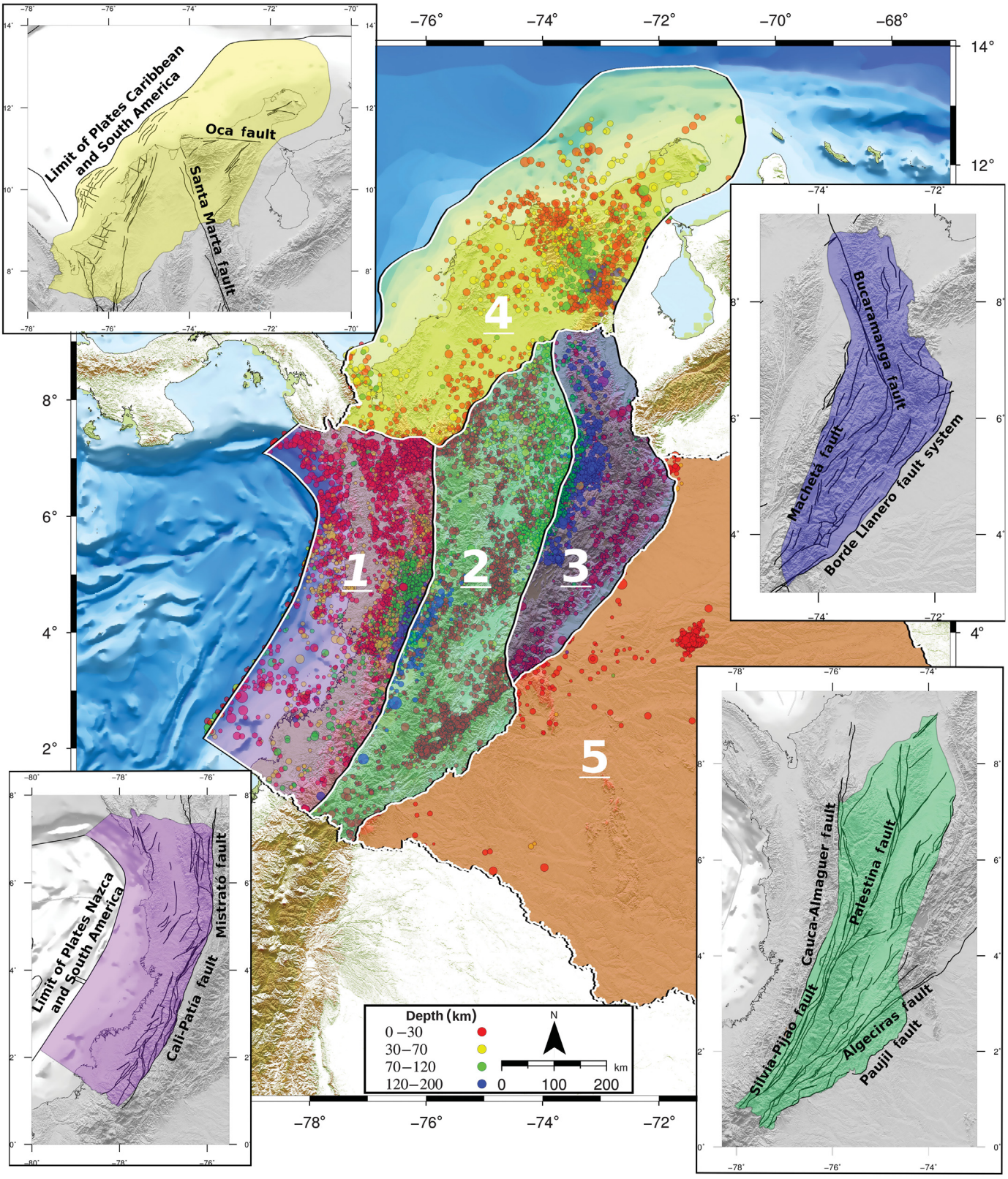

Cauca-Almaguer fault systems, and on the east by the Paujil fault and the border of the middle Magdalena valley. The southern boundary is the Colombian political border with Ecuador, whereas northern limit is the geomorphological change because of the central mountain range (see bottom

Figure 1. Map with the division of Colombian territory for M_L calibration with all seismicity used in this study. The small maps show the area for zones 1, 2, 3, and 4 with the principal fault systems used as boundaries. There are no principal fault systems in zone 5. Bottom left: zone 1, bottom right: zone 2, top right: zone 3, and top left: zone 4.

TABLE 1
Summary of Earthquakes Used in the Analysis

Zone	Stations	Events	Period	Size A*	Size x*	Size y*
1	15	5,454	January 2015–August 2017	81,811 × 5,471	5,471	81,811
2	31	6,153	January 2015–August 2017	190,744 × 6,186	6,186	190,744
3	13	6,856	January 2017–August 2017	75,417 × 6,869	6,869	75,417
4	11	2,960	January 2012–August 2017	32,561 × 2,973	2,973	32,516
5	8	1,393	January 2012–August 2017	11,145 × 1,403	1,403	11,516

*Size of matrix **A** and vectors **x** and **y** used in data inversion for each zone.

right in Fig. 1). High-seismic attenuation values are related to the large magma chambers under the volcanic axes (Jiménez, 2003), which lead to the presence of partially fused crustal rocks and elevated temperatures.

- Zone 3: The eastern Cordillera is bounded on the east by the Borde LLanero fault system, on the west by the seismicity pattern of the Bucaramanga Nest (also taking into account the boundary proposed by Jiménez (2003), and on the north by the Colombian political border with Venezuela and the geomorphological change because of the eastern mountain range (see top right in Fig. 1). In terms of lithology, sedimentary rocks of marine origin predominate and are affected by Triassic–Jurassic volcanic bodies. This zone has lower attenuation values than zones 1 and 2 but higher attenuation values than zone 5 (Jiménez, 2003).
- Zone 4: The northern Colombian–Caribbean region has a challenging configuration, which has led to scientific discussions about its genesis and the nature of its seismic activity. To the west and north, it is bounded by the Caribbean faults that represent the contact between the Caribbean and South American plates, on the east by the Colombian political border with Venezuela, and on the south by the geomorphological change because of the three mountain ranges (see top left in Fig. 1). In general, in this area, there are igneous and metamorphic rocks with a pattern of isolated clusters of seismicity. Low attenuation in the northern part of the Colombian territory has been reported by Jiménez (2003).
- Zone 5: The eastern plain region is bounded on the west by the Paujil and Borde LLanero fault systems, and on the north, east, and south by the Colombian political borders with Venezuela, Brazil, and Peru, respectively. This zone includes basement rocks, Paleozoic metamorphic rocks, and Precambrian rocks covered by Cenozoic deposits (Gómez and Diederix, 2015). It is called the stable South American shield. This is an area of stable tectonic in which low-attenuation values are expected (de Souza and Mitchell, 1998).

EARTHQUAKE DATA

Most of the seismic activity in Colombia is associated with the subduction of the Nazca plate, with surface faults systems and the Bucaramanga nest. The tectonics are complex because of subduction and the collision between the Panama arc and South America (Farris *et al.*, 2011). This complexity supports our decision to divide the territory into zones, because fracturing of the rocks directly affects the attenuation of seismic waves. Finally, we group the seismicity and the most important faults (see Fig. 1).

Data were selected from the RSNC-SGC database based on the zones (Fig. 1). A total of 22,816 seismic events were selected and the numbers of events selected for each zone are shown in Table 1. Because of the large amount of seismicity in zone 3, only events from 2017 were selected to decrease the computational load of the inversion, whereas for zones 4 and 5, events from 2012 to 2017 were selected to achieve better results in the inversion. The events selected were recorded by at least four stations, had magnitudes greater than 1.0 and location errors (root mean square) smaller than 2.0.

In the RSNC-SGC, the SEISAN software (Havskov and Ottemoller, 1999) is used to measure the maximum amplitudes at stations in which the *S* phase and *Lg* waves are clear and not truncated or clipped.

The waveforms were prepared by deconvolving the instrument response and convolving the corrected frequency response of a Wood–Anderson seismograph with a natural period of 0.8 s, a damping constant of 0.7, and a static magnification of 2080 (Uhrhammer and Collins, 1990). Then, a seismologist scanned them for the maximum amplitudes. These displacement amplitudes were measured in nanometers on the vertical component (Z) stored in the RSNC-SGC database. These data represent the main input for our study. Each amplitude value is associated with the hypocentral distance between the event and the station at which it was measured.

To ensure the quality of data used in the inversions, we used a filter based on the differences between measured amplitudes and the theoretical value calculated according to Rengifo and Ojeda (2004). The amplitudes with differences greater than 0.5 in $\log(A)$ were excluded from the study (see Fig. 2). This filtering process removed discrepancies because of human error and possible errors in the response files of the instruments.

METHODOLOGY

According to Richter (1935), the size of earthquakes can be represented using M_L defined as

$$M_I = \log A - \log A_0 + S, \quad (1)$$

in which A is the average of maximum amplitude in millimeters on the two horizontal components of a Anderson and Wood (1925) seismograph; $-\log A_0$ represents the distance-correction function using the original assumption that when a maximum amplitude of 1 mm is measured at a distance of 100 km the local magnitude is equal to 3; and S is a station correction.

The distance-correction function is defined based on the geometrical spreading, anelastic attenuation of the medium and scattering; these three factors cause a decrease in amplitude as the waves travel away from an earthquake source. Initially, Richter (1935) proposed a tabulated calibration function $-\log A_0(\Delta)$ with Δ as the epicentral distance. This classic calibration agrees with new attenuations determined using very large databases (e.g., Kanamori, 1983; Bakun and Joyner, 1984; Hutton and Boore, 1987), except for near-source distances in which Richter's calibration has low-quality results. The latter calibrations agree in that they separate the attenuation into two terms and represent the distance-correction function as

$$-\log A_0 = a \times \log(r/r_{\text{ref}}) + b \times (r - r_{\text{ref}}) + K(r_{\text{ref}}), \quad (2)$$

in which a is related to the geometrical spreading, b is the anelastic attenuation factor, r is the hypocentral distance, r_{ref} is a reference distance, and $K(r_{\text{ref}})$ is the base level or the reference magnitude. Rewriting equation (1) using (2) gives:

$$M_{\text{l}} = \log A + a \times \log(r/r_{\text{ref}}) + b \times (r - r_{\text{ref}}) + K(r_{\text{ref}}) + S, \quad (3)$$

in which the amplitude is in millimeters and the distances are in kilometers.

The equation previously used by the RSNC (Rengifo and Ojeda, 2004) was equation (3) with $a = 1.019$, $b = 0.0016$, and $K(r_{\text{ref}}) = -1.79$.

Bormann (2012) suggested a standard formula that excludes the explicit use of r_{ref} and formulates $K(r_{\text{ref}})$ as a constant c (base-level scale) that represents a source region correction term, discussed further in the following. Equation (3) with the new formulation gives:

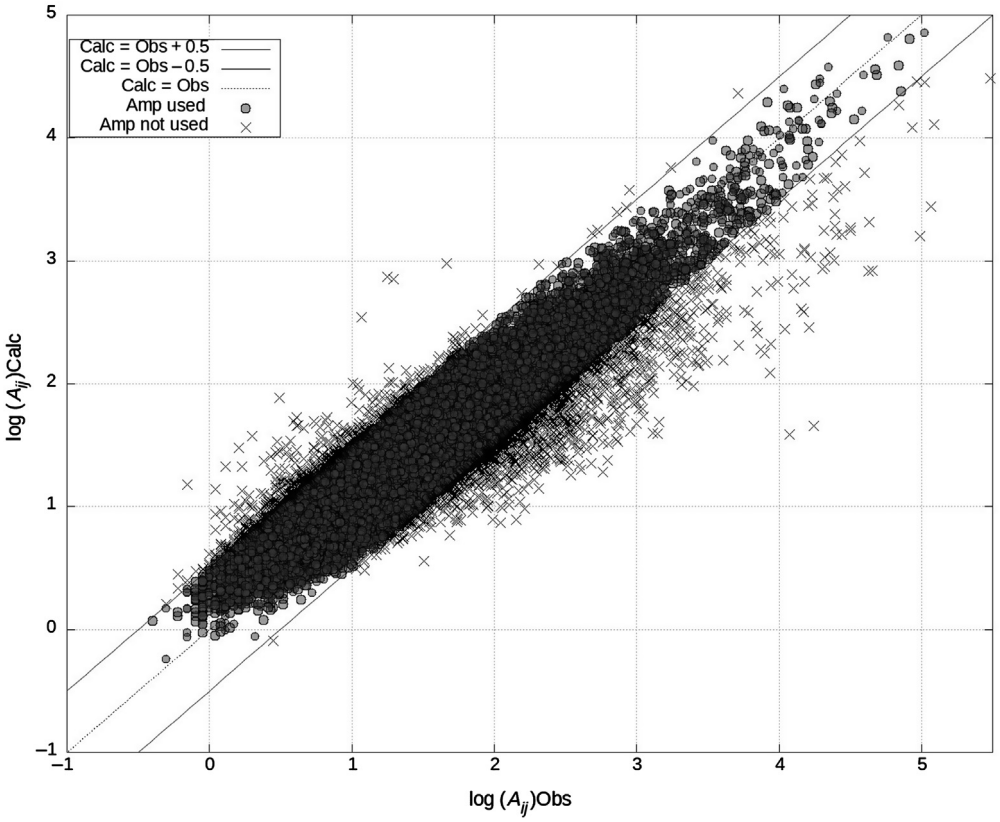

Figure 2. Measured (log(A_{ij})Obs) versus calculated (log(A_{ij})Calc) amplitudes. Solid lines show the boundaries used for filtering the amplitude dataset. Data outside the solid lines were excluded from the analysis.

$$M_{\text{L}} = \log A + a \times \log(r) + b \times r + c + S, \quad (4)$$

in which the amplitude is in nanometers and the distances are in kilometers. To avoid confusion, the local magnitude before the Bormann (2012) modification was represented by M_{l} and that after by M_{L}.

In this study, we use M_{L} in equation (4) instead of M_{l} in equation (3).

For a dataset with several events and stations, equation (4) can be rearranged as follows:

$$-a \times \log(r_{ij}) - b \times r_{ij} + \sum_{k=1}^{m} M_k \delta_{ik} - \sum_{l=1}^{n} S_l \delta_{lj} = \log A_{ij} + c,$$
$$i, k = 1, 2, \ldots m; \qquad j, l = 1, 2, \ldots n, \quad (5)$$

in which A_{ij} and r_{ij} are the maximum amplitudes and hypocentral distances for the ith event at the jth station, respectively, M_k is the magnitude of the kth event, S_l is the station correction for the lth station, δ_{ik} and δ_{lj} are the Kronecker delta for integers ik and lj, m is the number of events, and n is the number of stations.

By definition, the value of M_{l} in equation (3) must be equal to the base-level $K(r_{\text{ref}})$ for stations with $r = r_{\text{ref}}$. To

accomplish this, we use a constraint that the sum of all station corrections is equal to zero (Hutton and Boore, 1987):

$$\sum_{l=1}^{n} S_l = 0, \qquad l = 1, 2, \ldots n. \tag{6}$$

Equations (5) and (6) can be rewritten in matrix form as follows (Alsaker *et al.*, 1991; Langston *et al.*, 1998; Nguyen *et al.*, 2011):

$$\begin{bmatrix} p_{11} & q_{11} & 1 & 0 & \cdots & 0 & -1 & 0 & \cdots & 0 \\ p_{12} & q_{12} & 1 & 0 & \cdots & 0 & 0 & -1 & \cdots & 0 \\ \vdots & \vdots & & & \vdots & & & & \vdots & \\ p_{1n} & q_{1n} & 1 & 0 & \cdots & 0 & 0 & 0 & \cdots & -1 \\ p_{21} & q_{21} & 0 & 1 & \cdots & 0 & -1 & 0 & \cdots & 0 \\ p_{22} & q_{22} & 0 & 1 & \cdots & 0 & 0 & -1 & \cdots & 0 \\ \vdots & \vdots & & & \vdots & & & & \vdots & \\ p_{mn} & q_{mn} & 0 & 0 & \vdots & 1 & 0 & 0 & \cdots & -1 \\ 0 & 0 & 0 & 0 & \cdots & 0 & 1 & 1 & \cdots & 1 \end{bmatrix}_{(mn+1)\times(m+n+2)} \times \begin{bmatrix} a \\ b \\ M_1 \\ \vdots \\ M_m \\ S_1 \\ \vdots \\ S_1 \\ \vdots \\ S_n \end{bmatrix}_{(m+n+2)\times 1} = \begin{bmatrix} y_{11} \\ y_{12} \\ \vdots \\ y_{1n} \\ y_{21} \\ y_{22} \\ \vdots \\ y_{mn} \\ 0 \end{bmatrix}_{(mn+1)\times 1}, \tag{7}$$

in which $p_{ij} = -a \log(r_{ij})$, $q_{ij} = -b \times r_{ij}$, and $y_{ij} = \log A_{ij}$.

Rewriting the matrix as **A** and the two vectors as **x** and **y**, we can simplify equation (7) as

$$\mathbf{Ax} = \mathbf{y}, \tag{8}$$

which is a system of $(m \times n) + 1$ linearly independent equations. The vector **x** with $m + n + 2$ parameters to be determined represents the solution of our overdetermined inversion problem.

The data observed at a single station for each event yield the hypocentral distance r_{ij} and maximum amplitude A_{ij} to construct one row for **A** and **y**, respectively. Not all stations register all events. In this case, for each such station, a row must be added with r_i and A_{ij} equal to zero in **A** and **y**.

The sizes of matrix **A** and vectors **x** and **y** for the five zones in this study are given in Table 1.

To solve equation (8), we need to calculate the inverse of **A**. Because $m \neq n$, we use the generalized inverse matrix $\mathbf{A}^{-g}$ (e.g., Langston *et al.*, 1998; Nguyen *et al.*, 2011; Saunders *et al.*, 2013) through singular value decomposition (Menke, 1984):

$$\mathbf{x} = \mathbf{A}^{-g}\mathbf{Ax},$$

$$\mathbf{x} = \mathbf{A}^{-g}\mathbf{y}. \tag{9}$$

This methodology allows us to determine parameters a and b for each region, M_L by event and S by station. The only unknown parameter from equation (5) is c.

We decided to calculate the parameter c that we call the source region correction, which represents the base level of the magnitude scale at the reference distance. This parameter anchors the scale to Richter's original definition of local magnitude, although this connection has been modified by other authors. In Richter's original definition, a hypothetical Wood–Anderson seismograph at 100 km from the epicenter would record a maximum amplitude of 1 mm for an M_L 3 earthquake. Some authors have modified the reference distance and reference amplitude to be registered by the seismograph. Thus, Hutton and Boore (1987) changed the parameters to 17 km and 10 mm but did not modify the magnitude M_L 3. Others such as Alsaker *et al.* (1991) modified the reference distance and associated magnitude with 60 km and M_L 2.68 but did not change the maximum amplitude of 1 mm. Most authors prefer using hypocentral distance r instead of epicentral distance Δ.

We decided to retain the reference magnitude of M_L 3 and the hypocentral distance reference of 100 km, to connect our scale to Richter's original scale, but like most authors we realized that this assumption depends on the geographic region. Thus, we modified the maximum reference amplitude for each of our five zones. To calculate these amplitudes, we used the moment magnitude M_w, which is also calculated by the RSNC-SGC. We selected events in each zone with both types of calculated magnitudes M_w and M_L and then searched for stations with $r \approx 100$ km and $M_w \approx 3$. The maximum amplitudes measured on these events were averaged and used to satisfy the assumption. This method allowed us to build a scale connected to the original local magnitude scale and at the same time adapted to our territory.

RESULTS

The results of calibrations (parameters a and b in equation 4) after the zoning and the inversions are shown in Figures 3 and 4, and the equations for the calibrations for each zone are:

$$\text{Zone 1}: -\log A_0 - c_1 = 1.2448 \times \log(r) + 0.0024 \times r, \tag{10}$$

$$\text{Zone 2}: -\log A_0 - c_2 = 1.0563 \times \log(r) + 0.002 \times r, \tag{11}$$

$$\text{Zone } 3: -\log A_0 - c_3 = 1.0705 \times \log(r) + 0.0013 \times r, \quad (12)$$

$$\text{Zone } 4: -\log A_0 - c_4 = 1.2399 \times \log(r) + 0.0015 \times r, \quad (13)$$

$$\text{Zone } 5: -\log A_0 - c_5 = 0.7096 \times \log(r) + 0.0009 \times r. \quad (14)$$

Prior to this study, the magnitude values for events in zone 1 were underestimated by not accounting for the high attenuation of seismic waves associated with the subduction of the Nazca plate beneath the South American plate and with shallow fault systems.

In zone 4, high attenuation is also present. This feature is due to the contact between the Caribbean and South American plates. This contact, together with the shallow faults, is responsible for the seismic activity in this area.

As expected, the attenuation of seismic waves in zone 5 is low due to tectonic stability in this area. This characteristic is also reflected in the low level of seismic activity.

Base-level constraint (parameter *c*): Following the methodology discussed previously, we calculated the value of parameter *c* for each zone. The parameters of the analysis and results are presented in Table 2.

The trimmed means (means after discarding 20% of data at the high and low ends) for all amplitudes in each zone and the means for all hypocentral distances in each zone are shown in Table 2. All the values meet the anchorage condition. The amplitudes measured for events with magnitude close to 3.0 in all zones are lower than the value originally proposed by Richter. The closest value to the original amplitude of 1 mm is found in zone 4 with 0.7 mm, and the values deviating the most correspond to zones 1, 3, and 5 with less than 0.5 mm. These differences have three causes. First, we used the hypocentral distance rather than the epicentral distance as Richter did. Second, the attenuation in the zone described by Richter differs from that in our territory. Third, in the RSNC, the amplitudes are measured in the horizontal components, whereas Richter used the vertical components.

Including parameter *c*, the calibrations for each of the zones are:

$$\text{Zone } 1: -\log A_0 = 1.2448 \times \log(r) + 0.0024 \times r - 2.05, \quad (15)$$

$$\text{Zone } 2: -\log A_0 = 1.0563 \times \log(r) + 0.002 \times r - 1.760, \quad (16)$$

$$\text{Zone } 3: -\log A_0 = 1.0705 \times \log(r) + 0.0013 \times r - 1.531, \quad (17)$$

$$\text{Zone } 4: -\log A_0 = 1.2399 \times \log(r) + 0.0015 \times r - 2.178, \quad (18)$$

$$\text{Zone } 5: -\log A_0 = 0.7096 \times \log(r) + 0.0009 \times r - 0.690. \quad (19)$$

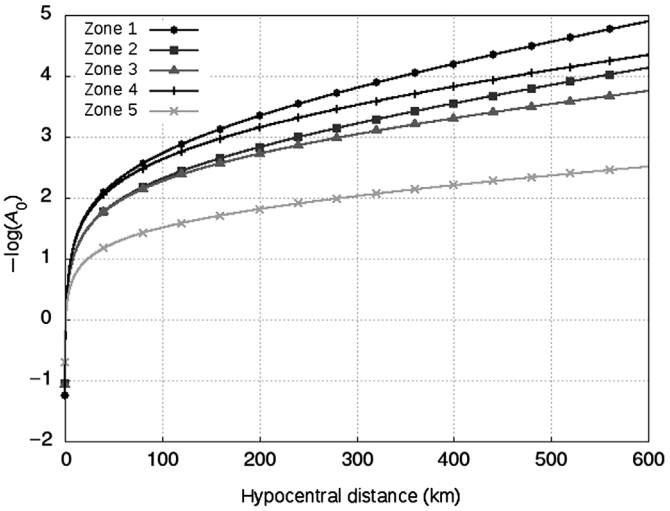

Figure 3. Calibrations ($-\log(A_0)$) versus hypocentral distance for the five zones without base-level constraint or the parameter *c*, calculated using equations (10)–(14).

In Figure 5, it is possible to see the difference in the magnitude estimates between those calculated with the calibration results of this work (Mag_{New}) and those previously calculated by the RSNC-SGC (Rengifo and Ojeda, 2004) (Mag_{Old}).

It is important to clarify that in Figures 3 and 4, the calibrations are presented without parameter *c*. In these figures, only parameters *a* and *b* (equation 4) are used, whereas for Figure 5, the calibrations with parameters *a*, *b*, and *c* presented in equations (15)–(19) are used.

Despite having different coefficients *a* and *b*, the magnitudes in zones 2 and 4 are very similar to those calculated with the calibration previously used by the RSNC-SGC. These results occur because the correction ($-\log A_0$) in equations (16) and (18) is similar to the correction previously used.

For zones 1, 3, and 5, the average magnitude difference is close to 0.5. Zones 1 and 3 have the highest seismicity in the country; therefore, this difference of 0.5 in magnitude is the most common discrepancy encountered when the RSNC-SGC catalog is compared with international lists.

Figure 5c shows the differences in $M_w - M_L$ using M_L previously calculated by the RSNC-SGC (old), and calculating M_L as proposed here for each zone (new). For zones 1 and 3, it is very clear that the difference between values of M_L and M_w decreases when using the results presented here. These magnitude differences decrease in most of the cases to almost 0 when the results of this work are used. The improvement in the agreement between M_w and M_L shows that the new local magnitude values provide a better estimate of the true release of energy from seismic events.

The decreases in the difference $M_w - M_L$ for zones 2 and 4 are smaller than those in zones 1 and 3 but still significant. The values for these zones are close to 0.3.

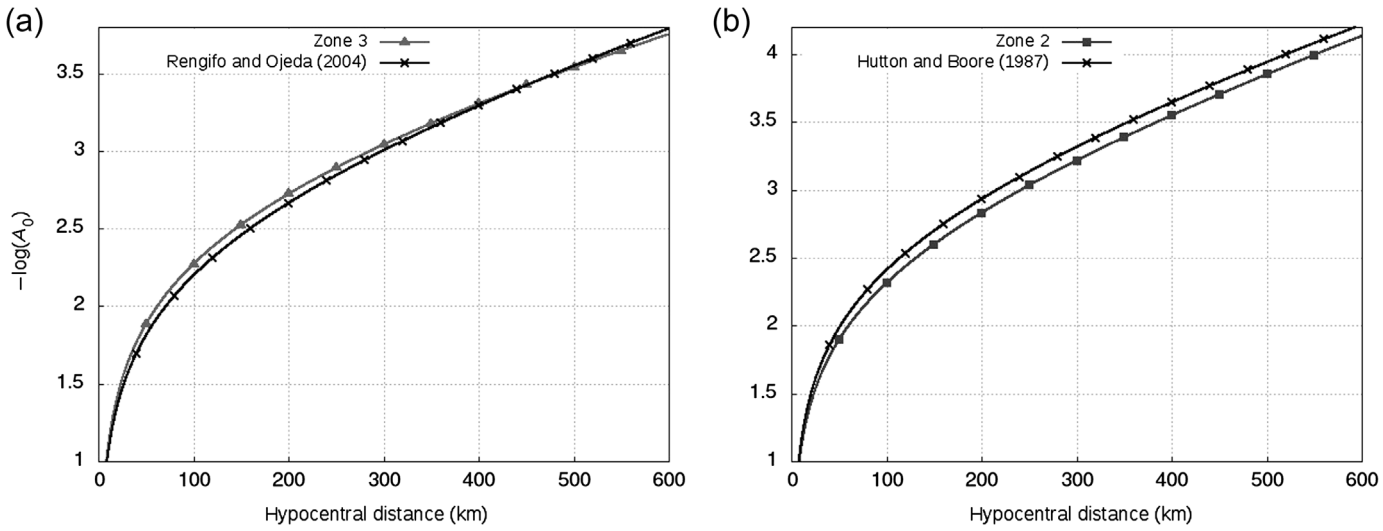

Figure 4. (a) Comparison of the calibration of zone 3 with that previously used by the Colombian National Seismic Network—Colombian Geological Survey (RSNC-SGC) from Rengifo and Ojeda (2004).(b) Comparison of the calibration of zone 2 with that proposed by Hutton and Boore (1987).

Zone 5 exhibits strange behavior; the difference between the two types of magnitude changes from close to 0.3 (using the previous calibration by Rengifo and Ojeda, 2004) to −0.2 (using the calibration results from this work). Therefore, the values of M_L calculated with the new calibration for zone 5 are slightly larger than M_w. This difference is perhaps due to a bias in the calculation of the attenuation parameters a and b and the anchoring parameter c because not many data and stations are available for this area.

DISCUSSION

The difference between our results for zone 4 and those of Ambeh and Lynch (1993), Ugalde *et al.* (2002), and Jiménez (2003) is due to the areas and events that were used. Ambeh and Lynch (1993) worked with events from the eastern Caribbean subduction zone; these data were seldom used in our work. On the other hand, Jiménez (2003) only used events from the southern part of zone 4. However, only a detailed study of the spatial variation of the attenuation in which the effects of intrinsic and scattering attenuation can be separated would allow us to distinguish the geological conditions that cause the decrease in wave amplitudes.

The five calibrations are different from each other. These differences highlight the importance of zoning the Colombian territory and the fact that seismic waves attenuate differently in each zone. The results show a clear decrease in the attenuation from west to east; (Fig. 3), with zone 1 having the greatest attenuation and zone 5 with the lowest attenuation.

There is a clear similarity between the calibrations for zone 3 presented and that done by Rengifo and Ojeda (2004) previously used by the RSNC-SGC throughout the Colombian territory (see Fig. 4). It shows that although Rengifo and Ojeda (2004) used events located throughout the Colombian territory, this calibration is strongly influenced by earthquakes located in the Bucaramanga nest. This bias generates discrepancies in local magnitude for events located in the other zones.

The result for zone 2 is similar to that proposed by Hutton and Boore (1987). Because the latter is one of the most accepted calibrations, this similarity supports the results presented here (see Fig. 4).

TABLE 2
Determination of Base-Level Constraint

Zone	Stations	Amplitude (mm)*	σ (mm)†	Hypocentral Distance (km)‡	σ (km)†	Parameter c
1	52	0.346	0.046	113	27	$c_1 = -2.05$
2	149	0.534	0.116	105	28	$c_2 = -1.76$
3	196	0.25	0.064	134	20	$c_3 = -1.53$
4	21	0.7	0.127	103	32	$c_4 = -2.18$
5	10	0.367	0.076	84	14	$c_5 = -0.69$

*Trimmed mean from all amplitudes.
†Standard deviation of amplitudes and hypocentral distances.
‡Mean from all hypocentral distances.

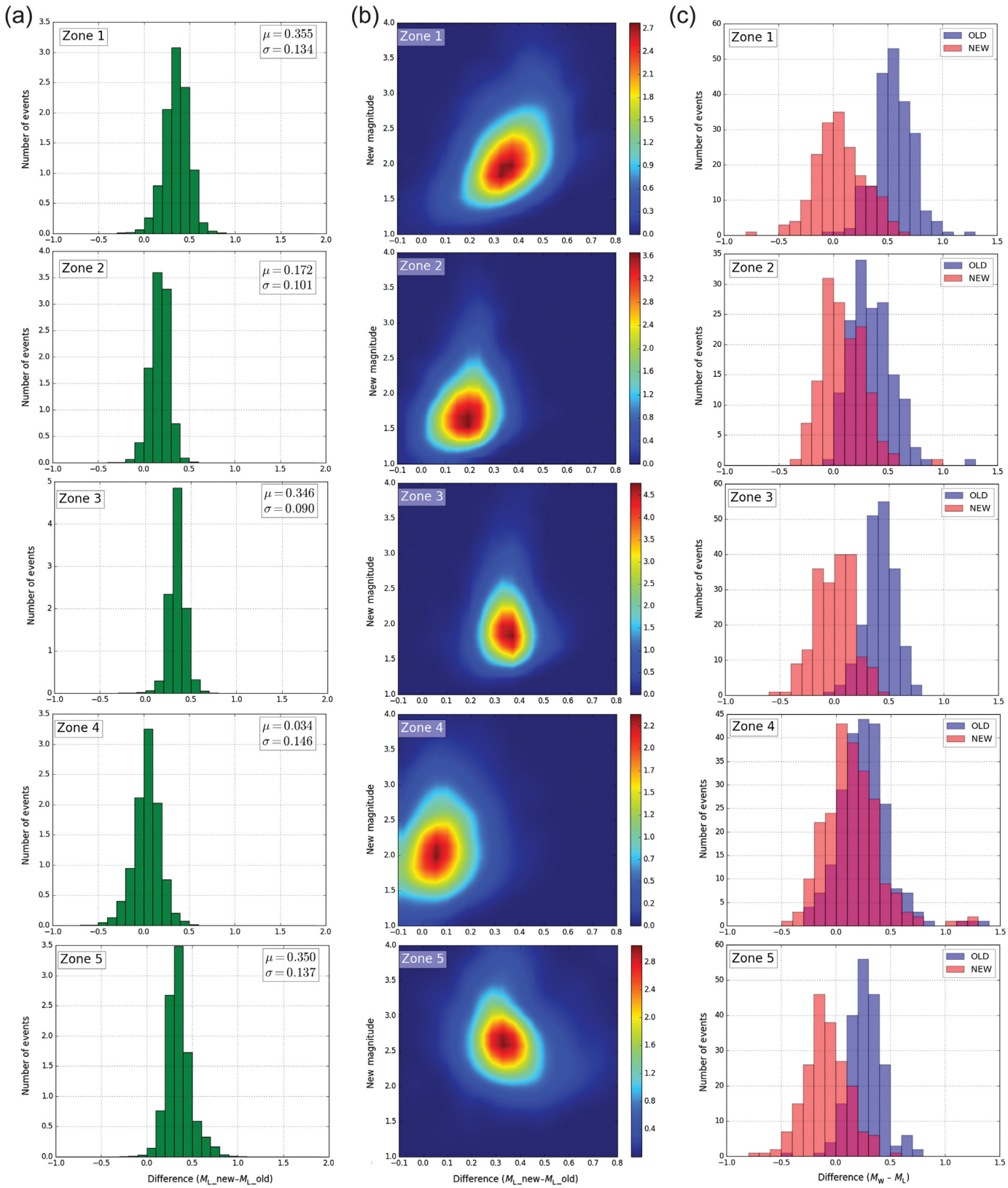

The division of the Colombian territory into zones with different equations for local magnitude has some implications for the RSNC-SGC.

The equation corresponding to each zone is associated with all the stations located in it. The stations near the boundaries

Figure 5. (a) Difference between local magnitudes calculated in this work (M_L new) and those previously calculated by the RSNC-SGC (M_L old) versus the normalized number of events. The mean and standard deviation are presented. (b) Difference between M_L new and M_L old versus M_L new, color bar shows the normalized number of events. (c) Difference between M_W—M_L new and M_W—M_L old versus number of events.

between zones use the two corresponding equations. Therefore, one event may have up to five different local magnitudes (M_{Ln}, in which $n = 1, \ldots, 5$) according to how many stations located in different zones recorded the earthquake. To obtain the final value, a summary magnitude from all available types is used for automatic locations, whereas for manual locations, the operator can choose between the summary magnitude or one of the types M_{Ln} according to the events location.

Since September 2018, the equations resulting from this work are being used by the RSNC-SGC. These new values of local magnitude show changes with respect to those stored in the catalog before this date. To achieve uniformity in the values of local magnitude for the entire catalog, the RSNC-SGC could systematically recalculate the local magnitudes using the new equations. In the case in which the RSNC-SGC does not have the necessary information (amplitudes) for this procedure, regressions between Mag_Old and Mag_New must be generated for each zone to recalculate the magnitudes.

Colombian seismicity has continuity with those in neighboring countries, especially Ecuador and Venezuela. There are no specific local magnitude equations for stations outside the national territory. It would be advisable to coordinate efforts with these countries to extend the results of this work. This would allow the uniform calculation of local magnitude. Currently, comparisons between the local magnitudes calculated in Colombia and those calculated by neighbors do not have an established procedure.

CONCLUSIONS

- To improve the estimates of local magnitude for earthquakes in Colombia, it was necessary to divide the territory into zones. This requirement was due to the different attenuation values associated with the various tectonic environments and regional geological features present in the country.
- New values of M_L calculated using the results of this work are close to the true release of energy from seismic events. This conclusion is supported by the decrease in the differences between values of M_w and M_L.
- Calculating the parameter c with the methodology proposed in this work allows us not only to anchor the new scale to the original M_L defined by Richter but also to bring the new scale closer to the M_w values calculated for events in our territory.
- The similarity between the calibration results in zone 3 and those previously used by the RSNC-SGC shows the bias caused by the use of the large number of events with hypocenters located in the Bucaramanga nest. This bias skews the values of local magnitude determined for events in the other zones of Colombia.
- In general, local magnitude values had been underestimated for the entire Colombian territory before using the equations presented here; for this reason, the RSNC-SGC must recalculate these magnitudes to improve uniformity in the databases.
- Although the results of our research are promising, a detailed study of the spatial variation of attenuation throughout the Colombian territory would allow more precise definition of areas and determination of the reasons that attenuation decreases from the subduction toward the stable South American shield.

DATA AND RESOURCES

Amplitudes and station information used in this study were collected from the database of the Servicio Geologico Colombiano. Data can be obtained by e-mail request to official accounts shared in the main page (www.sgc.gov.co). Maps were made using the Generic Mapping Tools version 5.5.18 (v.5.5.18; http://gmt.soest.hawaii.edu/). The data processing was done with the SeisComP3 software (www.seiscomp3.org). Some codes were developed using ObsPy, a Python package for seismology (www.pypi.org/project/obspy/). The main data inversion was made using the MATLAB software (www.mathworks.com). All websites were last accessed in May 2020.

ACKNOWLEDGMENTS

The authors would like to thank to the Servicio Geológico Colombiano (SGC) and in particular all staff of the National Seismological Network (RSNC-SGC) and tectonic group for providing the necessary data used in this research. This study was funded by the SGC through the project "Evaluación y Monitoreo de la Actividad Sísmica." The authors sincerely thank the two anonymous reviewers and Editor-in-Chief Thomas L. Pratt who helped them to improve this article.

REFERENCES

Alsaker, A., L. B. Kvamme, R. A. Hansen, A. Dahle, and H. Bungum (1991). The M_L scale in Norway, *Bull. Seismol. Soc. Am.* **81,** no. 2, 379–398.

Ambeh, B., and L. Lynch (1993). Coda Q in the eastern Caribbean, West Indies, *Geophys. J. Int.* **112,** 507–516.

Anderson, J. A., and H. O. Wood (1925). Description and theory of the torsion seismometer, *Bull. Seismol. Soc. Am.* **15,** no. 1, 1.

Bakun, W. H., and W. Joyner (1984). The M_L scale in central California, *Bull. Seismol. Soc. Am.* **74,** 1827–1843.

Bormann, P. (2012). New manual of seismological observatory practice (NMSOP-2), in *IASPEI*, P. Bormann (Editor), GFZ German Research Centre for Geosciences, Potsdam, Germany, 1–77.

de Souza, J. L., and B. J. Mitchell (1998). *Lg* coda Q variations across South America and their relation to crustal evolution, *Pure Appl. Geophys.* **153,** no. 2, 587–612.

Farris, D., C. Jaramillo, G. Bayona, S. Restrepo-Moreno, C. Montes, A. Cardona, A. Mora, R. Speakman, M. Glascock, P. W. Reiners, and V. Valencia (2011). Fracturing of the Panamanian Isthmus during initial collision with South America, *Geology* **39,** no. 11, 1007–1010.

Gao, L. (1992). Physical meaning of the coda envelopes, *Volcanic Seismol.* **3,** 391–403.

Gómez, J., and H. Diederix (2015). Geological map of Colombia 2015, *Servicio Geológico Colombiano*, Vol. 1, scale 1:1,000,000, 1–2.

Hanks, T., and H. Kanamori (1979). Moment magnitude scale, *J. Geophys. Res.* **84,** 2348–2350.

Havskov, J., and L. Ottemoller (1999). Seisan earthquake analysis software, *Seismol. Res. Lett.* **70,** no. 5, 532.

Hutton, L. K., and D. M. Boore (1987). The M_L scale in southern California, *Bull. Seismol. Soc. Am.* **77,** no. 6, 2074.

Jiménez, C. A. V. (2003). *Propagación de ondas sísmicas y atenuación de ondas de coda en el territorio Colombiano, Colección Jorge Alvarez Lleras*, Academia Colombiana de Ciencias Exactas, Físicas y Naturales, Bogotá, Colombia (in Spanish).

Kanamori, H. (1983). Magnitude scale and quantification of earthquakes, *Tectonophysics* **93,** no. 3, 185–199.

Kanamori, H., and L. Rivera (2008). Source inversion of W phase: Speeding up seismic tsunami warning, *Geophys. J. Int.* **175,** 228–238.

Langston, C. A., R. Brazier, A. A. Nyblade, and T. J. Owens (1998). Local magnitude scale and seismicity rate for Tanzania, East Africa, *Bull. Seismol. Soc. Am.* **88,** no. 3, 712.

Londono, J. (2015). *Definición de fórmulas de magnitud local para el área del complejo volcánico cerro bravo-cerro machín, Colombia*, Informe Interno, Servicio Geológico Colombiano, Bogotá, Colombia, 1–12 (in Spanish).

Londono, J., and J. Raigosa (2016). *Determinación de fórmula de magnitud local para la zona del paletará*, Informe Interno, Servicio Geológico Colombiano, Bogotá, Colombia, 1–11 (in Spanish).

Londoño, J. M., and J. A. Romero (2017). Local magnitude scale for valle medio del Magdalena region, Colombia, *J. S. Am. Earth Sci.* **80,** 237–243 (in Spanish).

Menke, W. (1984). *Geophysical Data Analysis: Discrete Inverse Theory*, Academic Press, Cambridge, Massachusetts.

Nguyen, L. M., T.-L. Lin, Y.-M. Wu, B.-S. Huang, C.-H. Chang, W.-G. Huang, T. S. Le, and V. T. Dinh (2011). The first M_L scale for north of Vietnam, *J. Asian Earth Sci.* **40,** no. 1, 279–286.

Ojeda, A., and L. Ottemöller (2002). Q_{Lg} tomography in Colombia, *Phys. Earth Planet. In.* **130,** no. 3, 253–270.

Rengifo, F. A., and A. Ojeda (2004). Inversion de amplitudes de registros sísmicos para el cálculo de magnitud $M_L$en colombia, *Memorias I Congreso Latinoamericano de Sismología. II Congreso, Colombiano de Sismología. Armenia, Agosto 16 al 21*, Congress work without editorial, Armenia, Colombia (in Spanish).

Richter, C. F. (1935). An instrumental earthquake magnitude scale*, *Bull. Seismol. Soc. Am.* **25,** no. 1, 1.

Sato, H., and I. Sacks (1989). Anelasticity and thermal structure of the oceanic upper mantle: Temperature calibration with heat flow data, *J. Geophys. Res.* **94,** 5705–5715.

Saunders, I., L. Ottemöller, M. B. C. Brandt, and C. J. S. Fourie (2013). Calibration of an M_L scale for South Africa using tectonic earthquake data recorded by the South African National Seismograph Network: 2006 to 2009, *J. Seismol.* **17,** no. 2, 437–451.

Shyam, C., and M. Tim (2004). The effect of hydrate content on seismic attenuation: A case study for Mallik 2L-38 well data, Mackenzie delta, Canada, *Geophys. Res. Lett.* **31,** no. 14, 1–4.

Sokos, E. N., and J. Zahradnik (2008). ISOALA a Fortran code and a Matlab GUI to perform multiple-point source inversion of seismic data, *Comput. Geosci.* **34,** no. 8, 967–977.

Ugalde, A., C. Vargas, L. Beneit, and J. A. Canas (2002). Seismic coda attenuation after the $M_w = 6.2$ Armenia (Colombia) earthquake of 25 January 1999, *J. Geophys. Res.* **107,** no. B6, ESE 1-1–ESE 1-12, doi: 10.1029/2001JB000197.

Uhrhammer, R. A., and E. R. Collins (1990). Synthesis of Wood–Anderson seismograms from broadband digital records, *Bull. Seismol. Soc. Am.* **80,** no. 3, 702.

Wong, V. (2001). Attenuation of coda waves at the Tres Virgenes volcanic area, Baja California Sur, Mexico, *Bull. Seismol. Soc. Am.* **91,** 683–693.

Manuscript received 6 September 2019
Published online 2 June 2020